

# IDŐJÁRÁS

*Quarterly Journal of the Hungarian Meteorological Service*  
Vol. 119, No. 1, January – March, 2015, pp. 23–39

## Evaluation and gap filling of soil NO flux dataset measured at a Hungarian semi-arid grassland

Dóra Hidy<sup>1</sup>, László Horváth<sup>\*1</sup>, and Tamás Weidinger<sup>2</sup>

<sup>1</sup>*MTA-SZIE Plant Ecology Research Group, Szent István University,  
Páter K. u. 1, 2103 Gödöllő, Hungary*

<sup>2</sup>*Department of Meteorology, Eötvös Loránd University,  
Pázmány Péter sétány 1/A, 1117 Budapest, Hungary*

*\*Corresponding author E-mail: horvath.laszlo.dr@gmail.com*

*(Manuscript received in final form February 8, 2015)*

**Abstract**—Nitric oxide soil emission flux was measured by 2–2 parallel manual and auto dynamic chambers on hourly basis above a Hungarian semi-arid, sandy grassland between August 2012 and January 2014. The measured datasets covered 43–85% of time period depending on chambers. We applied a gap filling method based on multivariable analysis (Sigma Plot) combined with maximum likelihood method. Trend of gap filled dataset shows large peaks mostly in summer and early fall. When soil parameters are far from the optimum (dry, warm conditions), the fluxes are negligible. Application of manual chambers closed for longer period results in substantial positive bias in flux estimation compared to auto chambers as a consequence of measurement setup, different temperature, and drier soil conditions below the chamber. Mean fluxes applying permanently closed dynamic chambers are approximately three times higher compared to auto chambers:  $0.176 \pm 0.489 \text{ nmol m}^{-2} \text{ s}^{-1}$  and  $0.058 \pm 0.130 \text{ nmol m}^{-2} \text{ s}^{-1}$ , respectively.

*Key-words:* nitric oxide, soil emission, gap filling, nitrification, grassland, dynamic chamber

## 1. Introduction

As it is well-known, one of the most important natural sources of atmospheric nitric oxide (NO) is the soil nitrification-denitrification process. It has been recognized earlier that soil flux of NO is similar in magnitude to fossil fuel emission of NO<sub>x</sub> (Davidson and Kinglerlee, 1997). For this reason, NO plays key role both in biosphere–atmosphere N-balance and in biogeochemical cycle of nitrogen.

Rate of soil NO flux strongly depends on soil temperature and moisture (Smith *et al.*, 1998) and on soil aeration, inorganic N content, and pH (Bouwman, 1996; Cárdenas *et al.*, 1993; Pilegaard, 2013).

There have been several research projects aiming on one hand to establish the magnitude of emission rate of nitrogen oxides from soils (e.g., NOFRETETE, Kesik *et al.*, 2005; Pilegaard *et al.*, 2006), and on the other hand to involve the soil NO emission in the N-inventory (e.g., NitroEurope, Skiba *et al.*, 2009). An Integrated Project ÉCLAIRE (<http://www.eclairerfp7.eu/>) started in 2011, among others to study the effect of climate change on air pollution impacts. One of the main measurement tasks of this project was the continuous monitoring of soil NO emission at different types of land (forest, arable, grass). Among the tree European grass stations, Bugacpuszta (Hungary) was selected to monitor and report soil NO fluxes continuously for 17 months on hourly basis.

We applied parallel both so-called manual (permanently closed) and auto (closed only during short measurement period) chambers for continuous measurements. As it was established earlier (Yao *et al.*, 2009), the use of manual chamber for measuring soil fluxes has some disadvantages. One of the main disadvantages is caused by the permanently closed status of chambers preventing the surface from precipitation. On the other hand, the top of chamber is exposed to solar radiation continuously heating the chamber box inside, compared to auto chambers which are open out of measurement cycle. Lower moisture and higher temperature conditions inside the permanently closed chambers may generate systematic bias in flux calculation.

As a consequence of the malfunction and failure of sampling and monitoring equipments during our measurement period, the data covers only the 43–85% of the full time of measurement campaign for different chambers.

The aim of this paper is firstly to apply a statistical gap filling method to complete the dataset, and secondly to give a semi-quantitative estimation on the positive bias in soil NO fluxes caused by applying manual chambers.

## 2. Methodology

### 2.1. Measurement of soil NO fluxes

Measurements were carried out in Bugacpuszta, Hungary, above a grassland between August 2012 and January 2014. The climate is semi-arid temperate continental, the mean annual temperature is 10.7 °C, and the average yearly precipitation is around 550 mm. The region has sandy soil with high sand (79%) and low clay (13%) contents in the upper 10 cm soil layer. More detailed information of location and characteristics are described in *Horváth et al.* (2010); *Machon et al.* (2010; 2011; 2015). Two-two parallel manual (Chamber 1 and Chamber 2; V = 2 L, h = 5 cm) and automatic (Chamber 3 and Chamber 4; V = 6.8 L, h = 10 cm) dynamic chambers were applied. Automatic chambers (Ricambi, Milan) were settled at fix positions and were closed only for 10 minutes every hour during sampling allowing the surface to be exposed to solar radiation and precipitation out of sampling time. Two manual chambers, home made by pale grey plastic, were permanently closed. The two chambers were re-settled during bi-weekly station maintenances onto other collars among the 6 fixed ones in turn. All of four chambers were sampled for 10 minutes at a flow rate of 2 L min<sup>-1</sup> in sequence every hour all together for 40 minutes; in the remaining 20 minutes, concentration gradients were measured by a mast at different heights. Soil temperature and moisture were measured a few meters apart from the chambers by 105T thermocouple probes and CS616 water content reflectometers, at -5; -30 cm and -3; -30 cm depths, respectively. A computer controlled valve system was switched the different channels in turn. The output concentrations of nitric oxide and ozone were measured by HORIBA APNA-350E and APOA-350E gas monitors through teflon tubing. Input concentrations of these gases were estimated from gradient concentration measurements at 0.5 m height, at the beginning of the one-hour long measurement cycle.

NO flux was calculated according to *Meixner et al.* (1997). Chemical correction of rapid reaction of NO with ozone ( $\text{NO} + \text{O}_3 \rightarrow \text{NO}_2 + \text{O}_2$ ) was taken into account. Under steady-state conditions, the mass balance equation for NO can be written as follows (the photolysis rate of NO<sub>2</sub> inside the dark chambers was estimated to be zero):

$$F_f + F_m + F_{bl} + F_{gp} = 0, \quad (1)$$

where  $F_f$  is the soil flux,  $F_m$  is the difference between fluxes entering and leaving the chamber,  $F_{bl}$  is the term for the wall effect which was negligible because of the relatively short residence time of the gas mixture in the chamber, and  $F_{gp}$  is the loss of NO due to the chemical reaction with ozone. For detailed description of flux calculations refer to *Horváth et al.* (2006) and *Machon et al.* (2015).

## 2.2. Statistical gap filling method

As soil NO flux depends on soil moisture, temperature, and soil organic nitrogen content, we have taken into account the variation of soil flux as a function of these parameters for gap filling. In the lack of regular observations we supposed that chemical characteristics of soil did not changed significantly during the observation period.

There are different gap filling methods used in micrometeorological flux measurements (Papale, 2012) i) empirical (e.g., look up tables), ii) interpolation (e.g., mean diurnal variation), iii) artificial neural networks, iv) non-linear regressions, and v) process oriented models. Gap filling methodology has been applied for the long term eddy covariance dataset in most cases. A statistical–regression methodology for gap filling of the long term soil respiration measurements was constructed by Gomez-Casanovas *et al.* (2013).

Effects of soil temperature and moisture for soil NO fluxes are well investigated and described by Gaussian distributions (Luo *et al.*, 2013; Pilegaard, 2013). Based on these investigations and on the former analysis of soil fluxes in Bugacpuszta (Machon *et al.*, 2011), a nonlinear regression gap filling method was selected which consisted of different steps.

Firstly we analyzed the dependence of soil flux in the function of soil physical parameters. We have taken into account four parameters, namely the soil moisture measured at –3 and –30 cm and soil temperature measured at –5 and –30 cm depths as SWC1, SWC2, TS1, and TS2, respectively (Fig. 1). During the measurement period, a total of 4686 parallel measurements were taken when all of the 4 chambers were together in operation. The dependence of fluxes on physical parameters was tested only for these measurements ensuring the homogeneity. We supposed that shape of functions is the same for all the measuring plots (chambers).

According to the shape of these functions and on the basis of earlier observations at the same site (Machon *et al.*, 2011), we supposed a maximum shape, exponential functions for moisture ( $x_{\text{SWC}}$ ) and temperature ( $x_{\text{TS}}$ ) using the assumption of Gaussian distributions. Although the flux dependence on soil temperature is generally exponential, in our case the temperature often exceeded the 20 °C resulting in lower bacterial activity caused by the heat stress or by the extreme low humidity at higher temperature regimes. As the first step, Eq. (2) was used for the estimation of missing soil flux rates ( $F_f$ ):

$$F_f = a_{\text{SWC}} \cdot \exp \left[ -0.5 \cdot \left( \frac{x_{\text{SWC}} - x_{0_{\text{SWC}}}}{b_{\text{SWC}}} \right)^2 \right] + a_{\text{TS}} \cdot \exp \left[ -0.5 \cdot \left( \frac{x_{\text{TS}} - x_{0_{\text{TS}}}}{b_{\text{TS}}} \right)^2 \right]. \quad (2)$$

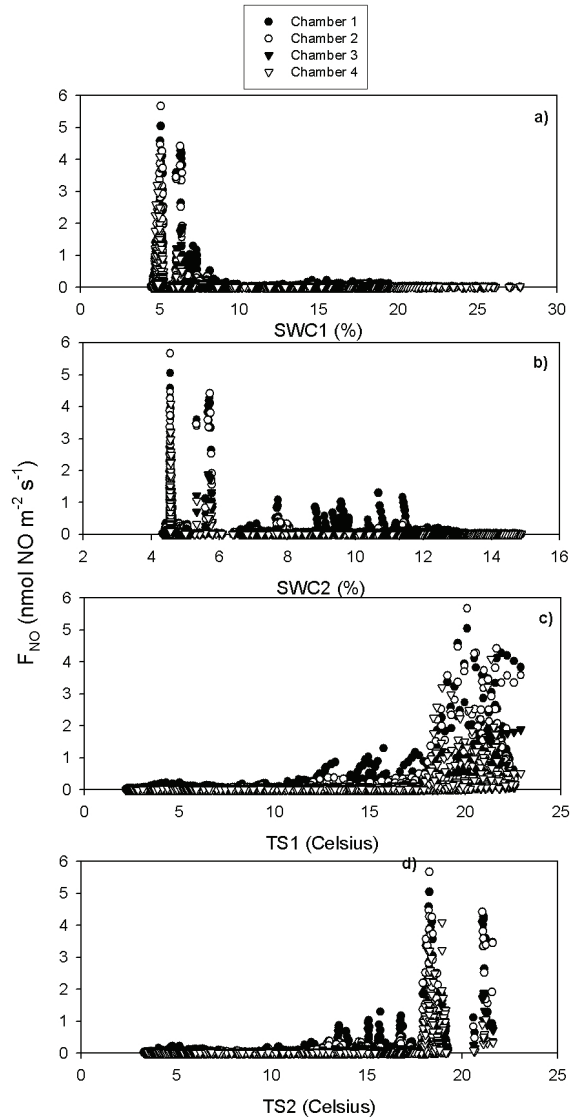


*Fig. 1.* NO fluxes measured by the four chambers in function of volumetric soil water content SWC1 (a), SWC2 (b) at  $-3$  and  $-30$  cm and soil temperature TS1 (c), TS2 (d) at  $-5$  cm and  $-30$  cm depths, respectively.

### 3. Results

#### 3.1. Gap filling of data series

We have calculated the dependence of NO flux in 4 different combinations of SWC and TS by the SigmaPlot 8.0 (Systat Software Inc., Chicago, USA) graphing and data analyses. (The Sigma Plot curve fitter uses the Marquardt-Levenberg algorithm). The best fit was observed among soil fluxes and SWC1-TS1 (*Fig. 2*) among hourly data on the days ( $n=4686$ ) when no measurement was missing (all chambers were in operation). Measured flux data

ranges within  $0\text{--}6 \text{ nmol m}^{-2} \text{ s}^{-1}$ . The relationship is significant at the probability level of  $p < 0.0001$  (except of two cases), and the calculated correlation coefficients are:  $R^2_{\text{Ch1}} = 0.435$ ;  $R^2_{\text{Ch2}} = 0.436$ ;  $R^2_{\text{Ch3}} = 0.393$ ;  $R^2_{\text{Ch4}} = 0.323$ . The standard errors (standard deviation of differences between the measured and estimated fluxes) of estimation are:  $\text{SD}_{\text{Ch1}} = 0.233$ ;  $\text{SD}_{\text{Ch2}} = 0.233$ ;  $\text{SD}_{\text{Ch3}} = 0.079$ ;  $\text{SD}_{\text{Ch4}} = 0.139 \text{ nmol m}^{-2} \text{ s}^{-1}$ .

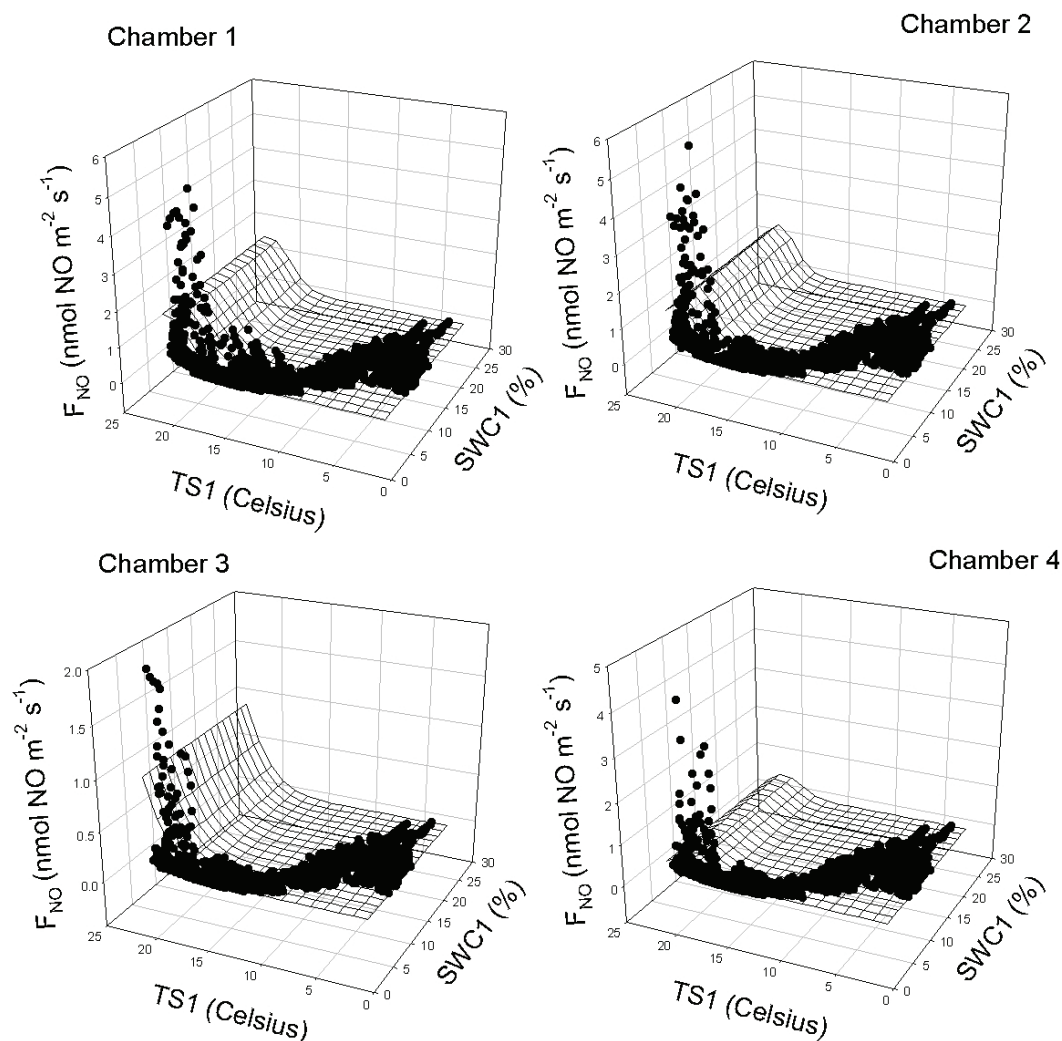


*Fig. 2.* Dependence of NO flux on soil properties (SWC at  $-3 \text{ cm}$  depth, TS at  $-5 \text{ cm}$  depth) measured by the different chambers. The fitted surface was calculated based on Eq. (2), the parameter estimation was created by Sigma Plot.

Further on, we have estimated the parameters of Eq. (2) by maximum likelihood method. There are various measures to express the distance between model and observation numerically (e.g., average, median, maximum, and normalized). It is difficult to clearly judge the significance of the different

quantitative measures, the choice of the misfit depends on the nature of the reference data (*Janssen and Heuberger, 1995*).

Hence, the NO flux estimation has two functions with 3–3 parameters for each chamber. In the next step, the parameter values were randomized for all chambers (Chamber 1–Chamber 4) to find the best combination of them. The measure of the goodness-of-fit is a special likelihood (Appendix Eq. A5.) taking simultaneously into account the correlation between the measured and modeled data, the average error, and the difference of the sum of measured and estimated data (see the equations in detail in the Appendix) (*Janssen and Heuberger, 1995*). The parameter values belonging to the maximum of the likelihood values are considered as the optimum parameter set.

After estimation for each chamber, the model was run with the optimum parameters compiled in *Table 1*. As the result of calibration, the correlation remained the same among measured and calculated data with parallel decrease of the error of estimation and the difference between measured and simulated sum (*Table 2*).

*Table 1.* Optimized parameters of Eq. (2)

	$a_{\text{SWC}}$	$b_{\text{SWC}}$	$x0_{\text{SWC}}$	$a_{\text{TS}}$	$b_{\text{TS}}$	$x0_{\text{TS}}$
Chamber 1	0.003	0.751	26.409	2.689	1.892	22.298
Chamber 2	0.050	0.227	48.252	2.060	1.571	21.399
Chamber 3	-1.524	-0.268	50.073	25.542	4.805	33.980
Chamber 4	2.134	0.073	3.068	1.044	1.813	21.505

*Table 2.* Coefficient of determination ( $R^2$ ), normalized error (NE,  $\text{nmol m}^{-2} \text{s}^{-1}$ ), and the difference between the measured and simulated sum (SE,  $\text{nmol m}^{-2} \text{s}^{-1}$ ), before (BC, Method 1) and after (AC, Method 2) calibration (n=4686)

	Chamber 1			Chamber 2			Chamber 3			Chamber 4		
	$R^2$	NE	SE	$R^2$	NE	SE	$R^2$	NE	SE	$R^2$	NE	SE
BC	0.44	1.36	-32.8	0.44	1.27	-28.8	0.39	1.52	-55.1	0.32	1.6	-20.1
AC	0.45	1.32	-1.82	0.45	1.26	0.74	0.37	1.58	6.55	0.29	1.1	10.9

The next step of gap filling procedure was the estimation of goodness of method. We analyzed the distribution of the data gaps. Each data series (Chambers 1–4) has 12,744 rows, with 15% to 57% of data lack depending on the chamber. We found that the most frequent length of the data gaps was 1, and the maximum was 689 in hour scale (*Fig. 3*).

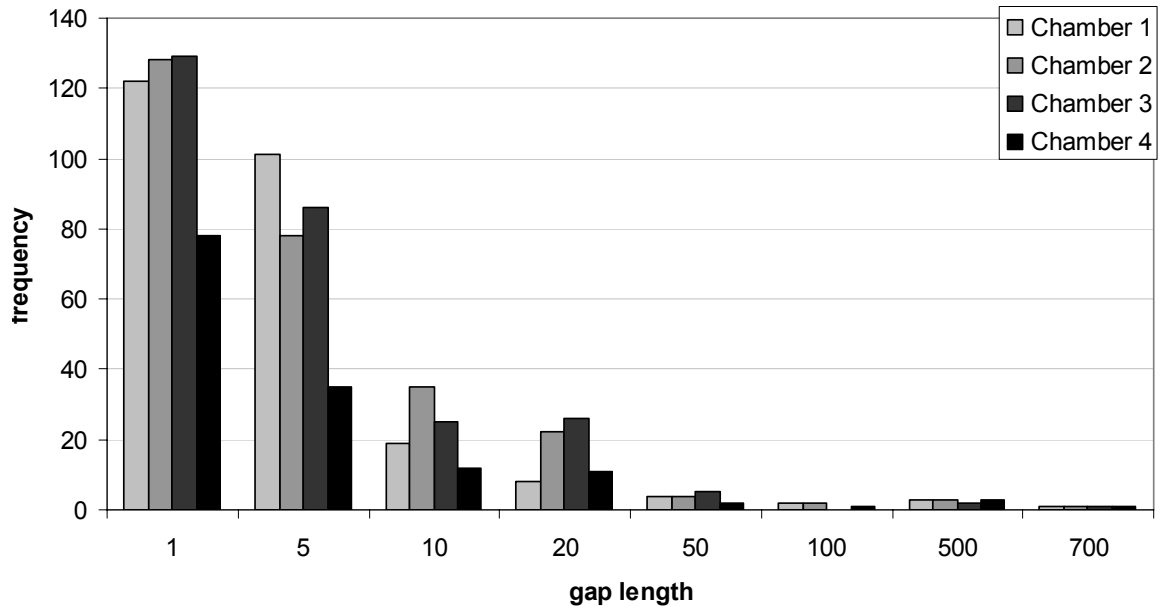


*Fig. 3.* Distribution of the data gaps (number of missing hourly data) regarding to the different chambers.

In order to examine the efficiency of gap filling methods, we created different numbers of data lacks in the measured data series by random number generator. *Table 3* contains the length and number of artificial gaps selected according to the original distribution of the data gaps (*Fig. 3*). The random gap creation was repeated 1000 times. The lacks were filled both by the simple method (Method 1: linear interpolation between the last data before the given gap and the first data after the given gap) and by the method described above (Method 2: using NO flux estimation based on SWC and TS data). The measured (NO flux data set without artificial gaps) and the estimated (artificial gaps are filled with estimated data) NO flux data were compared using likelihood values (function of the difference between the measured and estimated NO data defined by Eq. A5. in the Appendix) during random gap creation (1,000 random gap – 1,000 likelihood value). Hence, by the comparison of the two data series generated by the two methods (difference of the average likelihood), we found that in case of manual chambers, Method 1 gives better estimation (the difference is positive) if gap length is less than 10 hourly data and in case of automatic chambers, Method 1 is the better if gap length is less than 30. We can verify that we can use Method 2 for manual chambers in cases when gap length is longer than 10 and for automatic chambers in cases when gap length is longer than 30 (in other cases, Method 1 was used to fill the gaps) (*Fig. 4*).



Table 3. Length and number of artificial data gaps

name	length	number
G1	1	100
G5	5	100
G10	10	20
G20	20	10
G20	30	5
G50	50	5
G100	100	1
G500	500	1
G700	1000	1

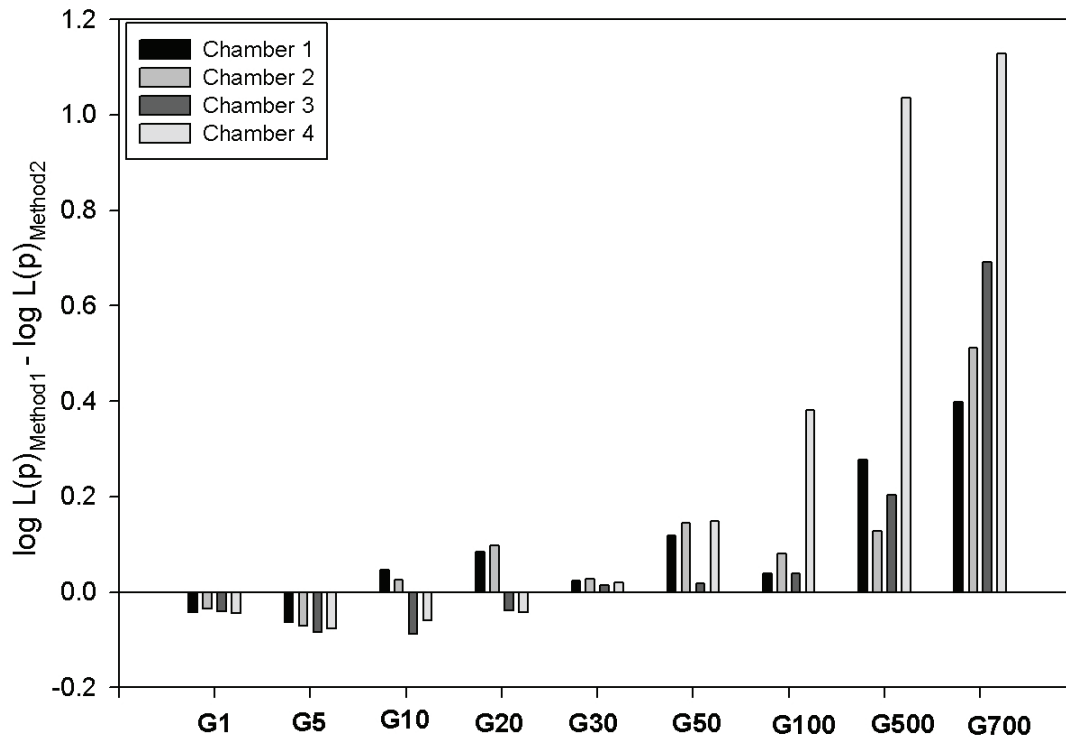


Fig. 4. The difference between the likelihood values using Method 1 and Method 2 during random gap creation in function of the gap length (G1: 1 data is missing, G5: five data are missing, etc.) for different chambers.

### 3.2. Evaluation of data

For evaluation, one dataset among 4 chambers was selected supposing that trend of NO flux is similar for all. The gap filled data series for Chamber 4 can be seen in Fig. 5. The trend of NO fluxes follows well the variation of soil wetness and temperature as it is expected. The optimum conditions for nitrification and

NO emission are in the dry and warm ranges. Two optimum periods occurred during summer/early fall during years of 2012 and 2013, when emission peaks appeared. In any other time period at either low temperature (lower than 10 °C) or high soil water content (higher than 10%), the NO production/emission are suppressed; the soil fluxes are negligible in magnitude compared to summer and early fall rates characterized by optimum soil conditions.

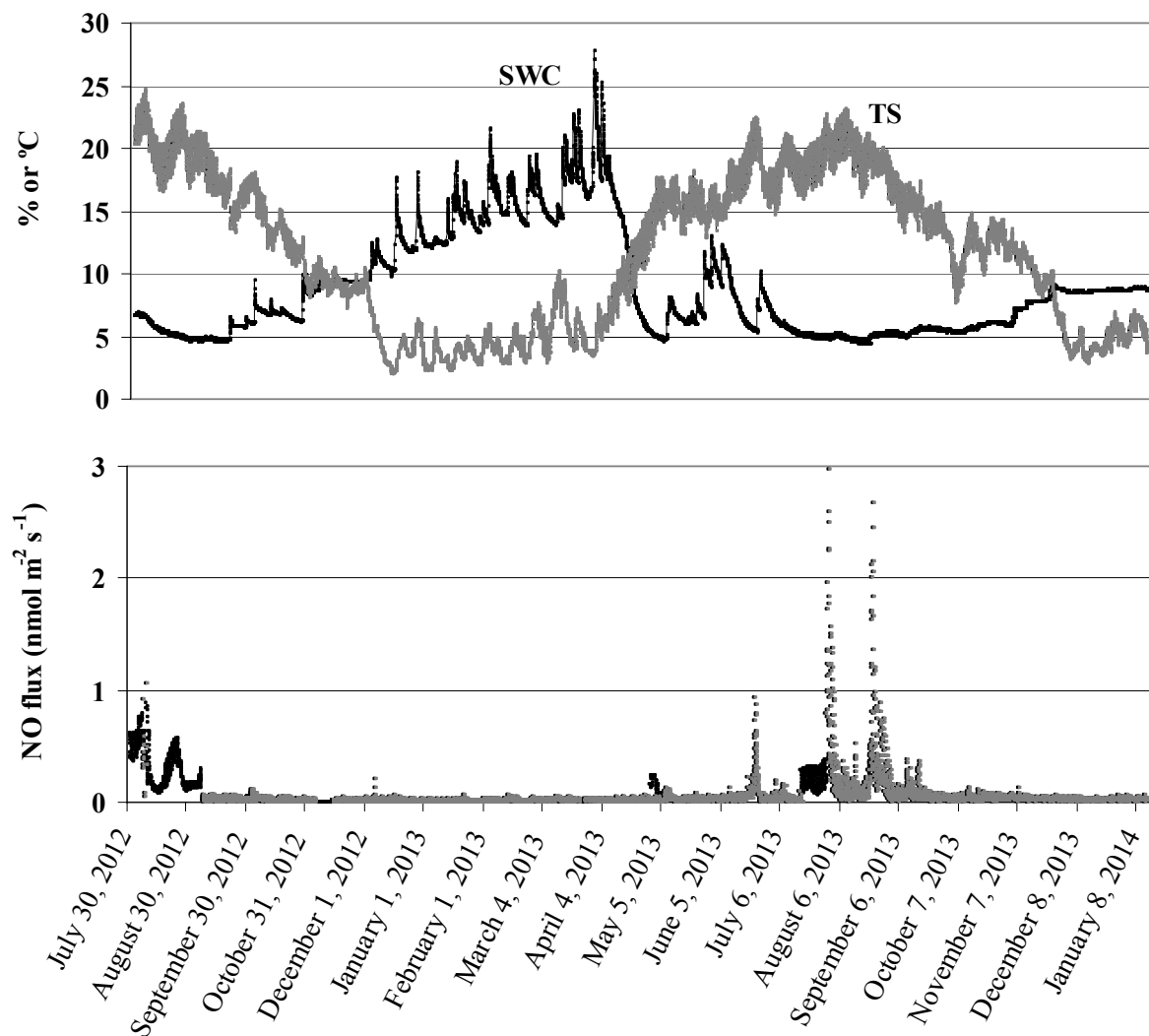


Fig. 5. Time course of soil properties, and measured (grey), and gap filled (black) NO fluxes for Chamber 4.

The statistical parameters of data series can be seen in *Table 4*. Gap filled flux data sets were compared to modeled ones for the whole period and for year 2013, separately. The agreement is acceptable for Chambers 1–3; the largest deviation

from the mean (less than 20%) appears for Chamber 4. Coefficients of variation (CV) for observed and calculated fluxes agree in magnitude for all chambers.

*Table 4.* Statistical parameters (mean, CV\*) of measured and gap filled datasets for soil NO flux ( $\text{nmol m}^{-2}\text{s}^{-1}$ )

	<b>Chamber 1</b>	<b>Chamber 2</b>	<b>Chamber 3</b>	<b>Chamber 4</b>
<b>Modeled, all</b>				
mean	0.168	0.183	0.062	0.065
CV	3.16	2.59	2.58	2.46
n	12 747	12747	12 747	12 747
<b>Gap-filled, all</b>				
mean	0.171	0.181	0.061	0.055
CV	3.04	2.54	2.41	2.05
n	12 747	12 747	12 747	12 747
<b>Modeled, 2013</b>				
mean	0.086	0.122	0.042	0.058
CV	2.88	2.21	2.65	2.82
n	8 760	8 760	8 760	8 760
<b>Gap-filled, 2013</b>				
mean	0.094	0.113	0.041	0.044
CV	2.11	1.93	1.94	1.92
n	8 760	8 760	8 760	8 760

CV\* (coefficient of variation): ratio of the sample standard deviation to the sample mean

### 3.3. Estimation of bias by using manual chambers

Mean of hourly soil NO fluxes were calculated separately for manual and auto chambers for cases when all of the 4 chambers were parallel in operation ( $n=4686$ ). The bulk daily course of ratio of fluxes measured by manual and auto chambers can be seen in *Fig. 6*. At night when solar radiation was zero, the average positive bias in fluxes measured by manual chambers (independently from the season) can be characterized by a factor of 1.6 as a consequence of drier soil conditions below the chamber. When solar radiation reached its maximum around the noon hours, the factor has increased up to 3.2. Mean flux values in *Table 4* also demonstrate a huge (around a factor of 3) increase in fluxes by applying permanently closed chambers. Because the magnitude of the

bias depends on many factors (climate, material and dimensions of chamber etc.), deeper conclusion can not be drawn out of this semi-quantitative estimation.

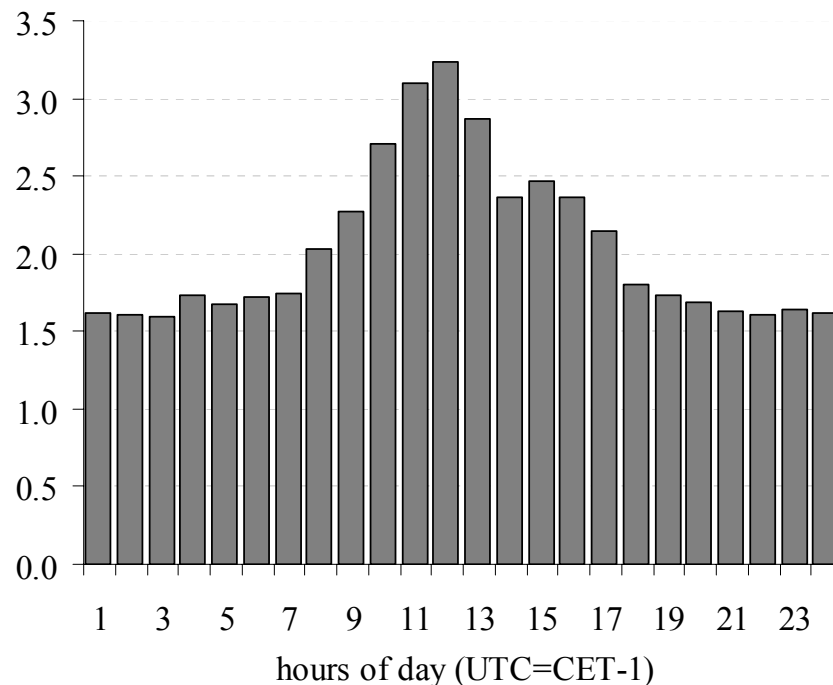


*Fig. 6.* Daily course of bias as ratio of measured soil NO flux by manual chambers compared to auto chambers (n=4686).

#### ***4. Conclusion***

Soil nitric oxide flux over sandy grassland strongly depends on soil moisture and temperature. Using the significantly correlated functions among fluxes, soil moisture, and temperature, the missing fluxes can be predicted. Analyzing the whole dataset we can establish that significant fluxes were measured when temperature and soil wetness were near to the optimum rate. In any cases, the fluxes were practically negligible. Expecting a drier and warmer climate in our region, reduction in soil NO emission is expected in the future.

The application of manual chambers (closed for longer period) for soil flux measurement may cause significant positive bias especially through the heating effect of solar radiation. The use of white chambers may reduce this effect, but the lid of chambers is an obstruction for precipitation that can not be prevented.

***Acknowledgements***—Authors acknowledge the financial support of Animal Change (FP7 266018), ÉCLAIRE (FP7 282910), NitroEurope (FP6) EU projects, MTA PD 450012 project, and PIAC 13-1-2013-0141 research and development project. Special thanks to Gyula Pávó, Zoltán Istenes, and Attila Eredics for their technical help.

## References

- Bouwman, A.F., 1996: Direct emission of nitrous oxide from agricultural soils. *Nutr. Cycl. Agroecosys.* 46, 53–70.
- Cárdenas, L., Rondón, A., Johansson, Ch., and Sanhueza, E., 1993: Effects of soil moisture, temperature, and inorganic nitrogen on nitric oxide emissions from acidic tropical savannah soils. *J. Geophys. Res.: Atmos.* 98, 14783–14790.
- Davidson, E.A. and Kinglerlee, W., 1997: A global inventory of nitric oxide emissions from soil. *Nutr. Cycl. Agroecosys.* 48, 37–50.
- Gomez-Casanovas, N., Anderson-Teixeira K., Zeri, M., Bernacchi, C.J., and DeLucia, E.H., 2013: Gap filling strategies and error in estimating annual soil respiration. *Glob. Change Biol.* 19, 1941–1952.
- Horváth, L., Führer, E., and Lajtha, K., 2006: Nitric oxide and nitrous oxide emission from Hungarian forest soils; linked with atmospheric N-deposition. *Atmos. Environ.* 40, 7786–7795.
- Horváth, L., Grosz, B., Machon, A., Tuba, Z., Nagy, Z., Czóbel, Sz., Balogh, J., Péli, E., Fóti, Sz., Weidinger, T., Pintér, K., and Führer, E., 2010: Estimation of nitrous oxide emission from Hungarian semi-arid sandy and loess grasslands, effect of soil parameters, grazing, irrigation and application of fertilizer. *Agric., Ecosys. Environ.* 139, 255–263.
- Janssen, P.H.M., and Heuberger, P.S.C., 1995: Calibration of process oriented models. *Ecol. Model.* 83, 55–66.
- Kesik, M., Ambus P., Baritz, R., Brüggemann, N., Butterbach-Bahl, K., Damm, M., Duyzer, J., Horváth, L., Kiese, R., Kitzler, B., Leip, A., Li, C., Pihlatie, M., Pilegaard, K., Seufert, G., Simpson, D., Skiba, U., Smiatek, G., Vesala, T., and Zechmeister-Boltenstern, S., 2005: Inventory of N<sub>2</sub>O and NO emissions from European forest soils. *Biogeosciences* 2, 353–375.
- Luo, G.J., Kiese, R., Wolf, B., and Butterbach-Bahl, K., 2013: Effects of soil temperature and moisture on methane uptakes and nitrous oxide emissions across three different ecosystem types. *Biogeosciences* 10, 3205–3219.
- Machon, A., Horváth, L., Weidinger, T., Grosz, B., Pintér, K., Tuba, Z., and Führer, E., 2010: Estimation of net nitrogen flux between the atmosphere and a semi-natural grassland ecosystem in Hungary. *Eur. J. Soil Sci.* 61, 631–639.
- Machon, A., Horváth, L., Weidinger, T., Pintér, K., Grosz, B., Nagy, Z., and Führer, E., 2011: Weather induced variability of N-exchange between the atmosphere and a grassland in the Hungarian Great Plain. *Időjárás* 115, 219–232.
- Machon, A., Horváth, L., Weidinger, T., Grosz, B., Mórting, A., and Führer, E., 2015: Measurement and modeling of N-balance between the atmosphere and the biosphere over a grazed grassland (Bugacpuszta) in Hungary. *Water Air Soil Poll.* 226:27.
- Meixner, F.X., Fickinger, Th., Marufu, L., Serca, D., Nathaus, F.J., Makina, E., Mukurumbira, L., and Andrae, M.O., 1997: Preliminary results on nitric oxide emission from a southern African savanna ecosystem. *Nutr. Cycl. Agroecosys.* 48, 123–138.
- Papale, D., 2012: Data gap filling. In (eds. Aubinet, M., Vesala, T., and Papale, D.), Eddy covariance. Springer, Dordrecht, Heidelberg, London, New York. 159–172.
- Pilegaard K., 2013: Processes regulating nitric oxide emissions from soils. *Phil. Trans. R. Soc. B* 368, 20130126.
- Pilegaard, K., Skiba, U., Ambus, P., Beier, C., Brüggemann, N., Butterbach-Bahl, K., Dick, J., Dorsey, J., Duyzer, J., Gallagher, M., Gasche, R., Horvath, L., Kitzler, B., Leip, A., Pihlatie, M.K., Rosenkranz, P., Seufert, G., Vesala, T., Westrate, H., and Zechmeister-Boltenstern, S., 2006: Factors controlling regional differences in forest soil emission of nitrogen oxides (NO and N<sub>2</sub>O). *Biogeosciences* 3, 651–661.
- Skiba, U., Jones, S.K., Drewer, J., Tang, Y.S., van Dijk, N., Helfter, C., Nemitz, E., Twigg, M., Famulari, D., Owen, S., Philatie, M., Vesala, T., Larsen, K.S., Carter, M.S., Ambus, P., Ibrom, A., Beier, C., Hensen, A., Frumau, A., Brüggemann, N., Gasche, R., Neftel, A., Spirig, C., Horvath, L., Freibauer, A., Cellier, P., Laville, P., Loubet, B., Magliulo, E., Bertolini, T., Seufert, G., Andersson, M., Manca, G., Laurila, T., Aurela, M., Zechmeister-Boltenstern, S., Kitzler, B., Schauffler, G., Siemens, J., Kindler, R., Flechard, C., Sutton, M.A., Erisman, J.W., Cape, J.N., and Butterbach-Bahl, K., 2009: Biosphere atmosphere exchange of reactive nitrogen

and greenhouse gases at the NitroEurope core flux measurement sites: Measurement strategy and first data sets. *Agr. Ecosys. Environ.* 133, 139–149.

Smith, K.A., Thomson, P.E., Clayton, H., McTaggart, I.P., and Conen, F., 1998: Effects of temperature, water content and nitrogen fertilisation on emissions of nitrous oxide by soils. *Atmos. Environ.* 32, 3301–3309.

Yao, Zh., Zheng, X., Xie, B., Liu, Ch., Mei, B., Dong, H., Butterbach-Bahl, K., and Zhu, J., 2009: Comparison of manual and automated chambers for field measurements of N<sub>2</sub>O, CH<sub>4</sub>, CO<sub>2</sub> fluxes from cultivated land. *Atmos. Environ.* 43, 1888–1896.

## *Appendix*

### *A1: Basic definitions*

*Error (E)*: difference between measured and simulated data on a given hour (i) using a given parameter set (p)

$$E_i = m_i(p) - d_i^{obs}$$

*Normalized bias (NB)*: normalized difference between the sum of model predictions and observed values

$$NB = \frac{\overline{M} - \overline{O}}{\overline{O}}$$

*Modeling efficiency*: a measure used to assess the predictive power of models (definition is identical to coefficient of determination (R<sup>2</sup>) in case of linear regression)

$$ME = 1 - \frac{\sum_i (E_i)^2}{\sum_i (d_i^{obs} - \overline{d_i^{obs}})^2}$$

*Log-likelihood*: it is more convenient to calculate with the natural logarithm of the likelihood

$$\log L(p) = \ln[L(p)]$$

### *A2. Likelihood and log-likelihood from Janssen median error misfit*

$$L(p)_{average} = \exp\left[-\left(\frac{1}{N} \sum_{i=1}^N NE_i\right)\right]$$

$$\log L(p)_{average} = -\left(\frac{1}{N} \sum_{i=1}^N NE_i\right)$$

*A3. Likelihood and log-likelihood from Janssen modeling efficiency error misfit*

$$L(p)_{efficiency} = \exp[-(ME)^{-1}]$$

$$\log L(p)_{efficiency} = -(ME)^{-1}$$

*A4. Likelihood and log-likelihood from Janssen bias misfit*

$$L(p)_{bias} = \exp[-NB]$$

$$\log L(p)_{bias} = -NB$$

*A5. Combined Likelihood and log-likelihood form*

$$L(p)_{combined} = L(p)_{average} \cdot L(p)_{bias} \cdot L(p)_{efficiency}$$

$$\log L(p)_{combined} = -\left(\frac{1}{N} \sum_{i=1}^N NE_i\right) + (-ME) + (-NB)$$